Supplemental material for:

Targeting a proteolytic neo-epitope on CUB-domain containing protein 1 (CDCP1) for RAS-driven cancers

Authors: Shion A. Lim[1]*‡, Jie Zhou[1]*, Alexander J. Martinko[1]§, Yung-Hua Wang[2,3], Ekaterina V. Filippova[4,5], Veronica Steri[3,6], Donghui Wang[3,6], Soumya G. Remesh[1], Jia Liu[1]¶, Byron Hann[6], Anthony A. Kossiakoff[4,5], Michael J. Evans[2,3], Kevin K. Leung[1], James A. Wells[1,7,8,#]

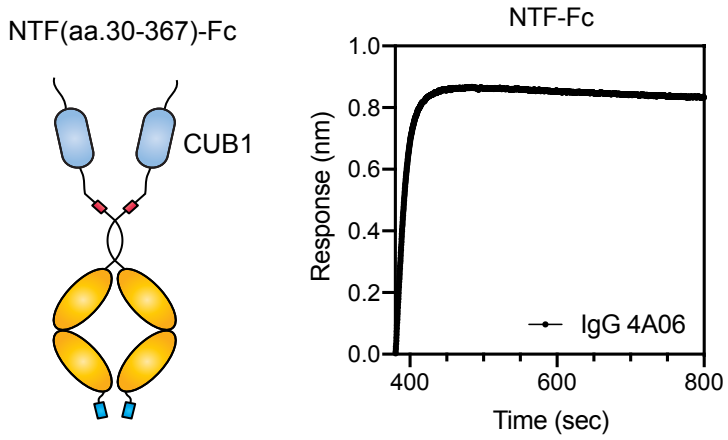

Supplementary Figure 1: BLI of IgG 4A06 binding to the N-terminal fragment (NTF) of CDCP1. NTF, composed of residues 30-367 of CDCP1, fused to a C-terminally biotinylated Fc domain was immobilized on Streptavidin-coated biosensors and probed with 25 nM of IgG 4A06. IgG 4A06 binds robustly to NTF-Fc, indicating that 4A06 recognizes an epitope within the NTF of the CDCP1 ectodomain.

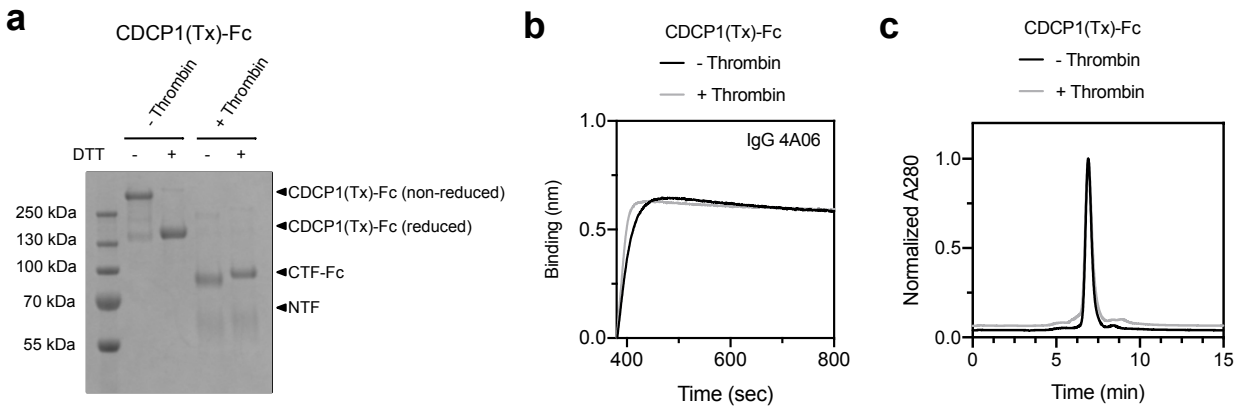

Supplementary Figure 2: Thrombin treatment of CDCP1 ectodomain with engineered thrombin cut site generates cleaved CDCP1 complex. (**a**) SDS-PAGE gel of Thrombin protease-cleavable CDCP1-Fc (CDCP1(Tx)-Fc). The reported R368/K369 cleavage site was replaced with a Thrombin protease recognition sequence $(GS)_5$-LVPRGS-$(GS)_5$. Treatment with Thrombin protease cleaves CDCP1(Tx)-Fc between the CUB1 and CUB2 domains and generate the corresponding NTF and CTF-Fc fragments. (**b**) BLI of IgG 4A06 binding to C-terminally immobilized CDCP1(Tx)-Fc treated or untreated with Thrombin shows that IgG 4A06, that recognizes the NTF, can still bind cleaved CDCP1. (**c**) SEC of CDCP1(Tx)-Fc treated or untreated with Thrombin protease shows that cleaved and uncleaved CDCP1 have similar elution profiles suggesting the NTF and CTF-Fc remain associated.

a **PL5 CDCP1 Peptide Coverage**

```
1   MAGLNCGVSI ALLGVLLLGA ARLPRGAEAF EIALPRESNI TVLIKLGTPT LLAKPCYIVI SKRHITMLSI KSGERIVFTF
81  SCQSPENHFV IEIQKNIDCM SGPCPFGEVQ LQPSTSLLPT LNRTFIWDVK AHKSIGLELQ FSIPRLRQIG PGESCPDGVT
161 HSISGRIDAT VVRIGTFCSN GTVSRIKMQE GVKMALHLPW FHPRNVSGFS IANRSSIKRL CIIESVFEGE GSATLMSANY
241 PEGFPEDELM TWQFVVPAHL RASVSFLNFN LSNCERKEER VEYYIPGSTT NPEVFKLEDK QPGNMAGNFN LSLQGCDQDA
321 QSPGILRLQF QVLVQHPQNE SNKIYVVDLS NERAMSLTIE PRPVKQSRKF VPGCFVCLES RTCSSNLTLT SGSKHKISFL
401 CDDLTRLWMN VEKTISCTDH RYCQRKSYSL QVPSDILHLP VELHDFSWKL LVPKDRLSLV LVPAQKLQQH THEKPCNTSF
481 SYLVASAIPS QDLYFGSFCP GGSIKQIQVK QNISVTLRTF APSFQQEASR QGLTVSFIPY FKEEGVFTVT PDTKSKVYLR
561 TPNWDRGLPS LTSVSWNISV PRDQVACLTF FKERSGVVCQ TGRAFMIIQE QRTRAEEIFS LDEDVLPKPS FHHHSFWVNI
641 SNCSPTSGKQ LDLLFSVTLT PRTVDLTVIL IAAVGGGVLL LSALGLIICC VKKKKKKTNK GPAVGIYNDN INTEMPRQPK
721 KFQKGRKDND SHVYAVIEDT MVYGHLLQDS SGSFLQPEVD TYRPFQGTMG VCPPSPPTIC SRAPTAKLAT EEPPPRSPPE
801 SESEPYTFSH PNNGDVSSKD TDIPLLNTQE PMEPAE
```

m/z	z	ppm	DB Peptide	Constant Mods	Variable Mods	RT	Score	Expect
926.9037	2	-1.4	IQKNIDCMSGPCPFGE	Carbamidomethyl@7; Carbamidomethyl@12		73.341615	32.6	8.9e-13
499.9567	3	-0.92	RAMSLTIEPRPVK			45.8198360	26.9	1.6e-11
468.0182	4	1.1	RAMSLTIEPRPVKQSR			38.2428570	27.6	4.2e-11
428.9924	4	0.045	RAMSLTIEPRPVKQS			45.6854540	25.9	7.3e-11
614.9983	3	3.0	ASRQGLTVSFIPYFKE			92.5646640	17.4	3.2e-9
614.2806	2	0.12	FVPGCFVCLE	Carbamidomethyl@5; Carbamidomethyl@8		108.28199	23.4	3.8e-9
658.0088	3	-2.9	ASRQGLTVSFIPYFKEE			93.2353870	25.4	1.2e-8
472.0164	4	0.043	RAMSLTIEPRPVKQSR		Oxidation@3	32.1087810	19.8	1.4e-8
690.8532	2	-1.1	SNKIYVVDLSNE			71.874420	27.2	3.9e-8
541.7657	2	-2.2	VDTYRPFQG			52.6320720	19.1	3.5e-7
678.3301	2	3.1	KFVPGCFVCLE	Carbamidomethyl@6; Carbamidomethyl@9		88.1169730	18.2	3.5e-7

b **PL45 CDCP1 Peptide Coverage**

```
1   MAGLNCGVSI ALLGVLLLGA ARLPRGAEAF EIALPRESNI TVLIKLGTPT LLAKPCYIVI SKRHITMLSI KSGERIVFTF
81  SCQSPENHFV IEIQKNIDCM SGPCPFGEVQ LQPSTSLLPT LNRTFIWDVK AHKSIGLELQ FSIPRLRQIG PGESCPDGVT
161 HSISGRIDAT VVRIGTFCSN GTVSRIKMQE GVKMALHLPW FHPRNVSGFS IANRSSIKRL CIIESVFEGE GSATLMSANY
241 PEGFPEDELM TWQFVVPAHL RASVSFLNFN LSNCERKEER VEYYIPGSTT NPEVFKLEDK QPGNMAGNFN LSLQGCDQDA
321 QSPGILRLQF QVLVQHPQNE SNKIYVVDLS NERAMSLTIE PRPVKQSRKF VPGCFVCLES RTCSSNLTLT SGSKHKISFL
401 CDDLTRLWMN VEKTISCTDH RYCQRKSYSL QVPSDILHLP VELHDFSWKL LVPKDRLSLV LVPAQKLQQH THEKPCNTSF
481 SYLVASAIPS QDLYFGSFCP GGSIKQIQVK QNISVTLRTF APSFQQEASR QGLTVSFIPY FKEEGVFTVT PDTKSKVYLR
561 TPNWDRGLPS LTSVSWNISV PRDQVACLTF FKERSGVVCQ TGRAFMIIQE QRTRAEEIFS LDEDVLPKPS FHHHSFWVNI
641 SNCSPTSGKQ LDLLFSVTLT PRTVDLTVIL IAAVGGGVLL LSALGLIICC VKKKKKKTNK GPAVGIYNDN INTEMPRQPK
721 KFQKGRKDND SHVYAVIEDT MVYGHLLQDS SGSFLQPEVD TYRPFQGTMG VCPPSPPTIC SRAPTAKLAT EEPPPRSPPE
801 SESEPYTFSH PNNGDVSSKD TDIPLLNTQE PMEPAE
```

m/z	z	ppm	DB Peptide	Constant Mods	Variable Mods	RT	Score	Expect
926.9037	2	-1.4	IQKNIDCMSGPCPFGE	Carbamidomethyl@7; Carbamidomethyl@12		73.341615	32.6	8.9e-13
499.9567	3	-0.92	RAMSLTIEPRPVK			45.8198360	26.9	1.6e-11
468.0182	4	1.1	RAMSLTIEPRPVKQSR			38.2428570	27.6	4.2e-11
428.9924	4	0.045	RAMSLTIEPRPVKQS			45.6854540	25.9	7.3e-11
614.9983	3	3.0	ASRQGLTVSFIPYFKE			92.5646640	17.4	3.2e-9
614.2806	2	0.12	FVPGCFVCLE	Carbamidomethyl@5; Carbamidomethyl@8		108.28199	23.4	3.8e-9
658.0088	3	-2.9	ASRQGLTVSFIPYFKEE			93.2353870	25.4	1.2e-8
472.0164	4	0.043	RAMSLTIEPRPVKQSR		Oxidation@3	32.1087810	19.8	1.4e-8
690.8532	2	-1.1	SNKIYVVDLSNE			71.874420	27.2	3.9e-8
541.7657	2	-2.2	VDTYRPFQG			52.6320720	19.1	3.5e-7
678.3301	2	3.1	KFVPGCFVCLE	Carbamidomethyl@6; Carbamidomethyl@9		88.1169730	18.2	3.5e-7

c **HPAC CDCP1 Peptide Coverage**

```
1   MAGLNCGVSI ALLGVLLLGA ARLPRGAEAF EIALPRESNI TVLIKLGTPT LLAKPCYIVI SKRHITMLSI KSGERIVFTF
81  SCQSPENHFV IEIQKNIDCM SGPCPFGEVQ LQPSTSLLPT LNRTFIWDVK AHKSIGLELQ FSIPRLRQIG PGESCPDGVT
161 HSISGRIDAT VVRIGTFCSN GTVSRIKMQE GVKMALHLPW FHPRNVSGFS IANRSSIKRL CIIESVFEGE GSATLMSANY
241 PEGFPEDELM TWQFVVPAHL RASVSFLNFN LSNCERKEER VEYYIPGSTT NPEVFKLEDK QPGNMAGNFN LSLQGCDQDA
321 QSPGILRLQF QVLVQHPQNE SNKIYVVDLS NERAMSLTIE PRPVKQSRKF VPGCFVCLES RTCSSNLTLT SGSKHKISFL
401 CDDLTRLWMN VEKTISCTDH RYCQRKSYSL QVPSDILHLP VELHDFSWKL LVPKDRLSLV LVPAQKLQQH THEKPCNTSF
481 SYLVASAIPS QDLYFGSFCP GGSIKQIQVK QNISVTLRTF APSFQQEASR QGLTVSFIPY FKEEGVFTVT PDTKSKVYLR
561 TPNWDRGLPS LTSVSWNISV PRDQVACLTF FKERSGVVCQ TGRAFMIIQE QRTRAEEIFS LDEDVLPKPS FHHHSFWVNI
641 SNCSPTSGKQ LDLLFSVTLT PRTVDLTVIL IAAVGGGVLL LSALGLIICC VKKKKKKTNK GPAVGIYNDN INTEMPRQPK
721 KFQKGRKDND SHVYAVIEDT MVYGHLLQDS SGSFLQPEVD TYRPFQGTMG VCPPSPPTIC SRAPTAKLAT EEPPPRSPPE
801 SESEPYTFSH PNNGDVSSKD TDIPLLNTQE PMEPAE
```

m/z	z	ppm	DB Peptide	Constant Mods	Variable Mods	RT	Score	Expect
926.9043	2	-0.67	IQKNIDCMSGPCPFGE	Carbamidomethyl@7; Carbamidomethyl@12		73.4511430	29.8	1.2e-10
571.6540	3	-0.087	RAMSLTIEPRPVKQS			45.89985	22.9	2.9e-9
690.8530	2	-1.3	SNKIYVVDLSNE			71.9418880	26.0	2.1e-8
802.1774	4	2.6	RAMSLTIEPRPVKQSRKFVPGCFVCLE	Carbamidomethyl@22;Carbamidomethyl@25		77.273185	17.9	5.3e-6
621.2883	2	0.70	YYIPGSTTNPE			69.5404680	15.7	1.0e-5
651.3331	3	0.38	RSGVVCQTGRAFMIIQE	Carbamidomethyl@6		72.552615	15.7	5.8e-5

Supplementary Figure 3: CDCP1 peptides identified by IP-MS of PDAC cell lines. Peptides identified by IP-MS of 3 different PDAC cell lines (a) PL5, (b) PL45, (c) HPAC. Peptides corresponding to cleaved fragments of CDCP1 were identified on PL5 and PL45 cells, but not HPAC.

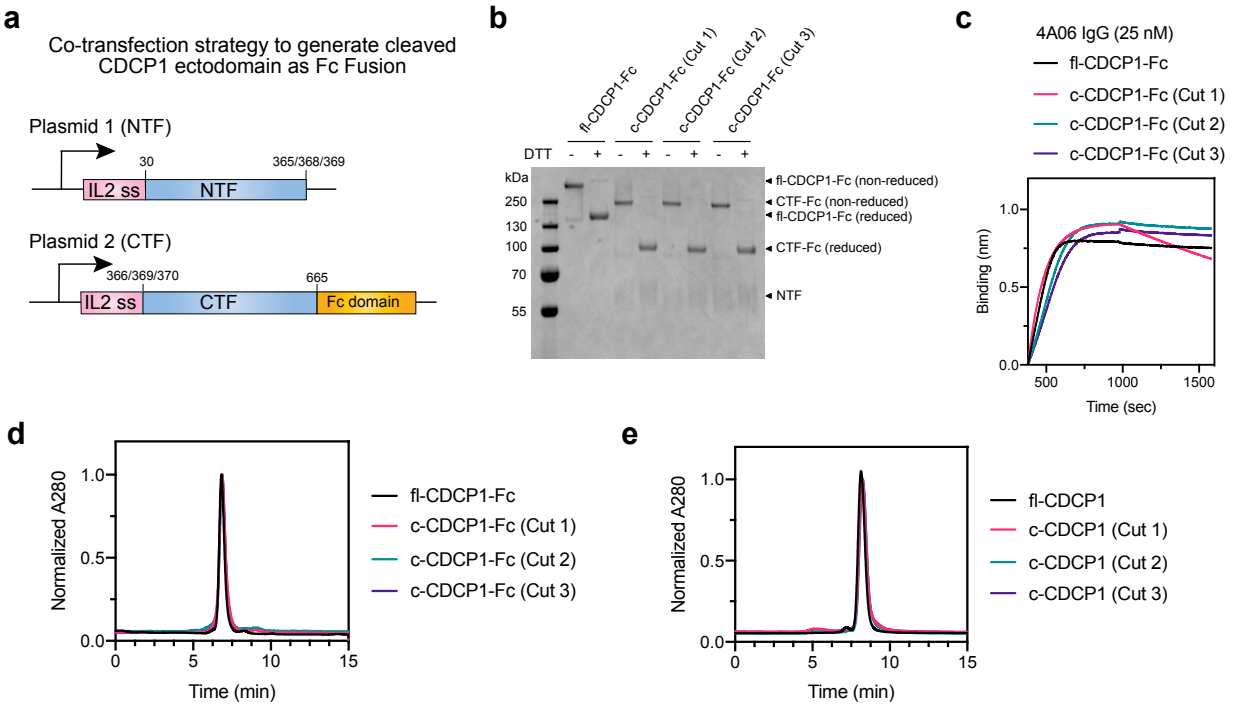

Supplementary Figure 4: Generation of fl-CDCP1 and c-CDCP1 ectodomain with endogenous cut sites. (**a**) Schematic of a two-plasmid co-transfection strategy to generate the cleaved CDCP1 ectodomain as an Fc fusion. The NTF and CTF-Fc were encoded on separate plasmids, with an IL2 signal sequence preceding each sequence. (**b**) SDS-PAGE gel of fl-CDCP1-Fc and c-CDCP1-Fc (Cut 1, Cut 2, Cut 3) (**c**) BLI shows robust binding of IgG 4A06 to fl-CDCP1-Fc and c-CDCP1-Fc. (**c**) BLI of IgG 4A06 to fl-CDCP1-Fc and c-CDCP1-Fc (Cut 1, Cut 2, Cut 3) show robust binding, indicating NTF is present on all 4 constructs. (**d**) SEC of fl-CDCP1-Fc and c-CDCP1-Fc (Cut 1, Cut 2, Cut 3) shows that all 4 antigens have similar elution profiles. (**e**) SEC of fl-CDCP1 and c-CDCP1 (Cut 1, Cut 2, Cut 3) without Fc domains shows that all 4 antigens have similar elution profiles.

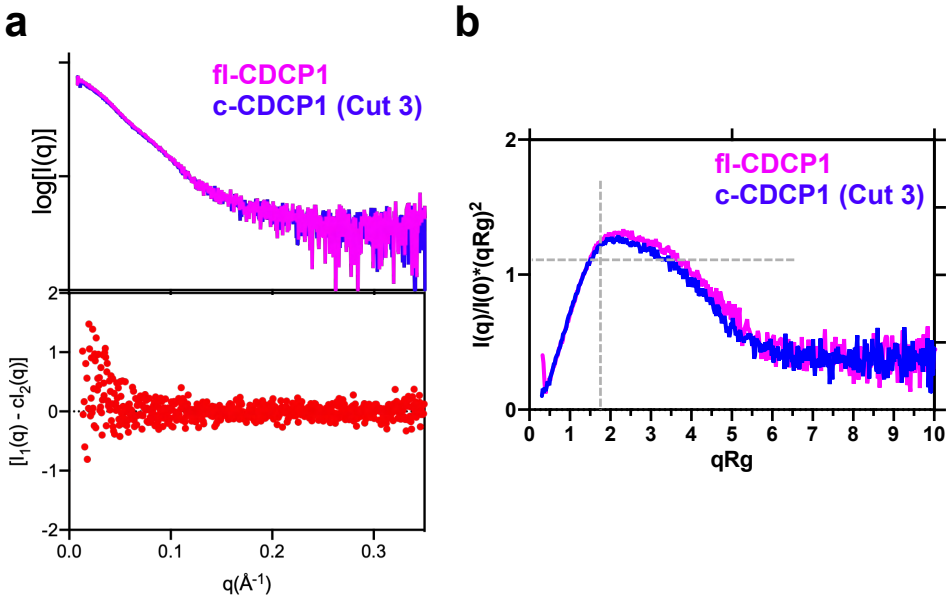

Supplementary Figure 5: SEC-SAXS of uncleaved and cleaved CDCP1 ectodomain show similar conformations. (**a**) SAXS profiles, (**b**) Normalized Kratky plot, and (**c**) P(r) function of fl-CDCP1 and c-CDCP1 (Cut 3) ectodomain indicates that there are no large-scale conformational changes between fl-CDCP1 and c-CDCP1.

Supplementary Table 1: SAXS and MALS experimental parameters

	R_g (Å)	Dmax (Å)	MW MALS/SAXS (kDa)
fl-CDCP1	45.4 +/- 0.6	145	97.0 (+/- 0.11%) / ~112
c-CDCP1 (Cut3)	44.1 +/- 0.5	143	99.6 (+/- 0.11%) / ~108

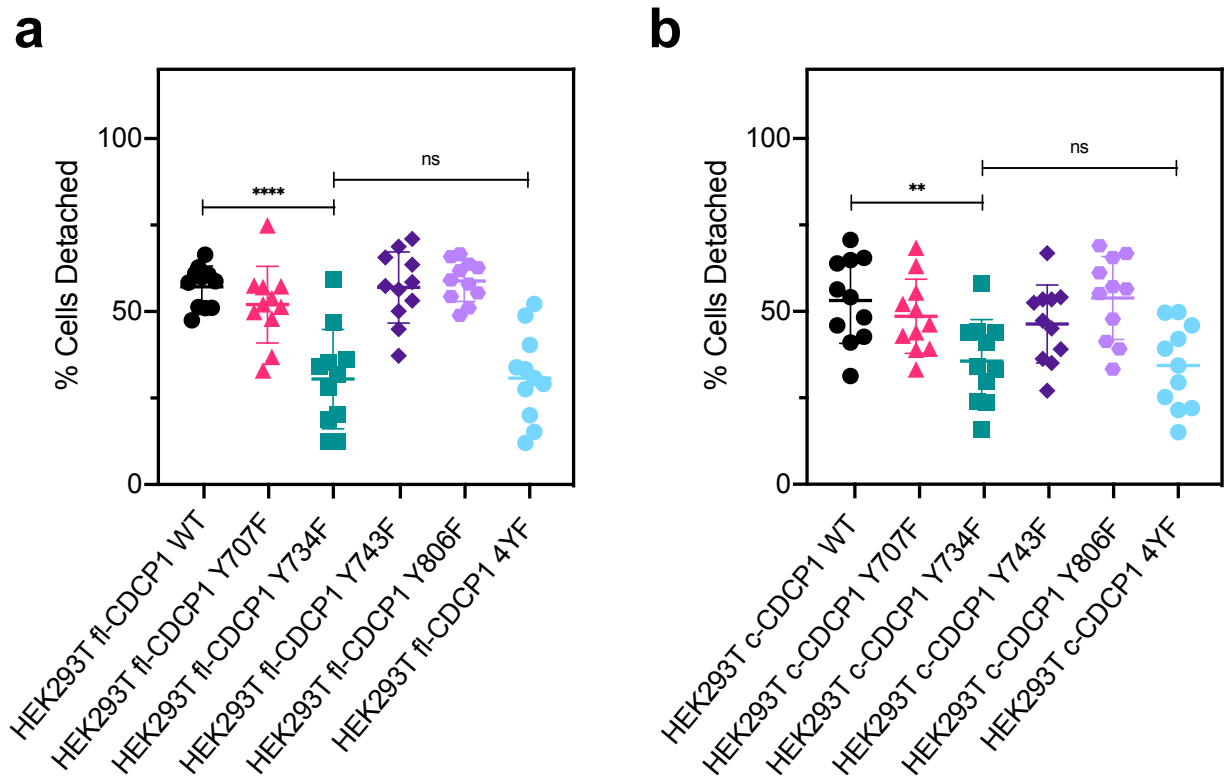

Supplementary Figure 6: Cell Adhesion Assay of HEK293T cells expressing CDCP1 tyrosine variants show that phosphorylation of Y734 is critical for detachment. Cell adhesion assay of for HEK293T cells expressing (**a**) fl-CDCP1 and (**b**) c-CDCP1 variants. The 4 intracellular tyrosine residues (Y707, Y734, Y743, Y806) were individually or altogether (4YF) mutated to phenylalanine to abrogate signaling. Data indicate that Y734 is important for CDCP1-associated intracellular signaling implicated in decreased cell adhesion. Data represent individual values and mean ± SEM. There was a significant difference in cell adhesion between the different cell lines expressing fl-CDCP1 variants ($F(6, 70) = 10.98$, $p < 0.0001$, one-way ANOVA) and c-CDCP1 variants ($F(5, 60) = 5.832$, $p < 0.0002$, one-way ANOVA). Tukey post-hoc tests revealed that the decreased cell adhesion resulting from overexpression of either fl-CDCP1 and c-CDCP1 was reversed when all 4 intracellular tyrosine residues (4YF) or specifically Y734F was mutated (****$p < 0.0001$ for fl-CDCP1 v. fl-CDCP1 Y734F, **$p = 0.011$ for c-CDCP1 v. c-CDCP1 Y734F). There was no significant difference between the Y734F and 4YF mutations, and there was no significant effect compared to wild-type when Y707, Y743, or Y806 was mutated ($p > 0.05$), suggesting that Y734 is the intracellular phosphorylation site responsible for modulating CDCP1-driven loss of cell adhesion.

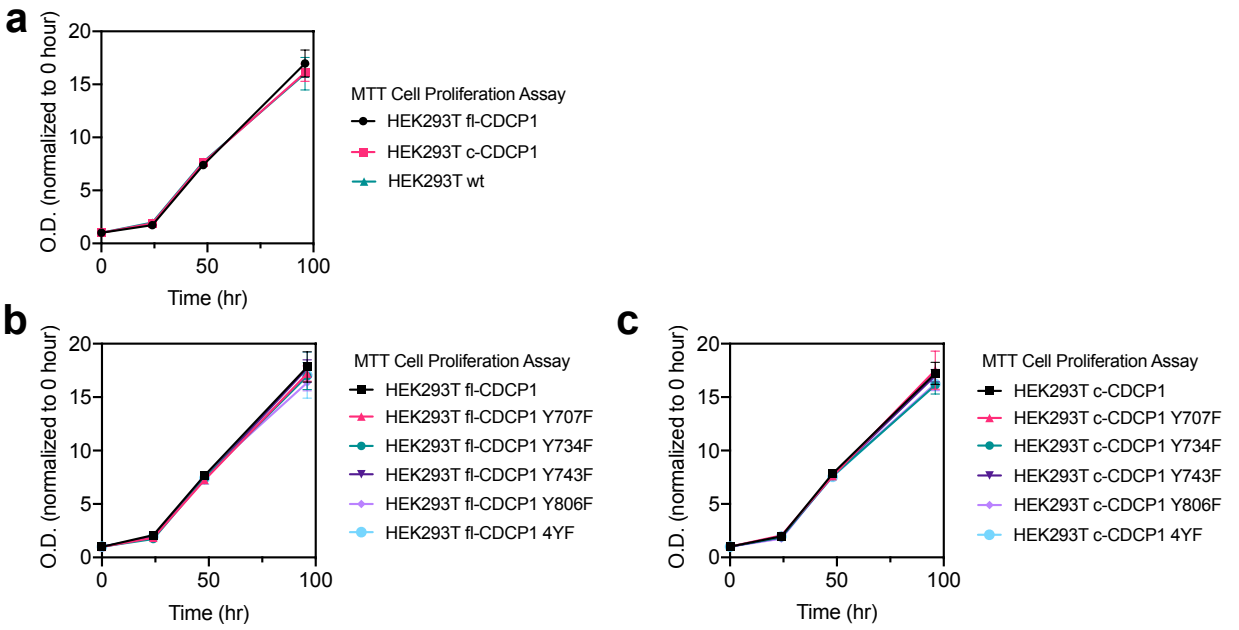

Supplementary Figure 7: MTT Cell proliferation assay of HEK293T cell lines expressing fl-CDCP1 and c-CDCP1 variants show over-expression, phosphorylation, or cleavage have no effect on cell proliferation. Cell proliferation assay measured by MTT for HEK293T cells expressing (**a**) HEK293T WT, fl-CDCP1, and c-CDCP1, (**b**) fl-CDCP1 variants, and (**c**) c-CDCP1 variants. fl-CDCP1 or c-CDCP1 overexpression does not have a significant effect on cell growth compared to HEK293T WT cells. All variants have similar rates of growth over a 4-day period. Data were collected in triplicate and average and standard deviation are shown.

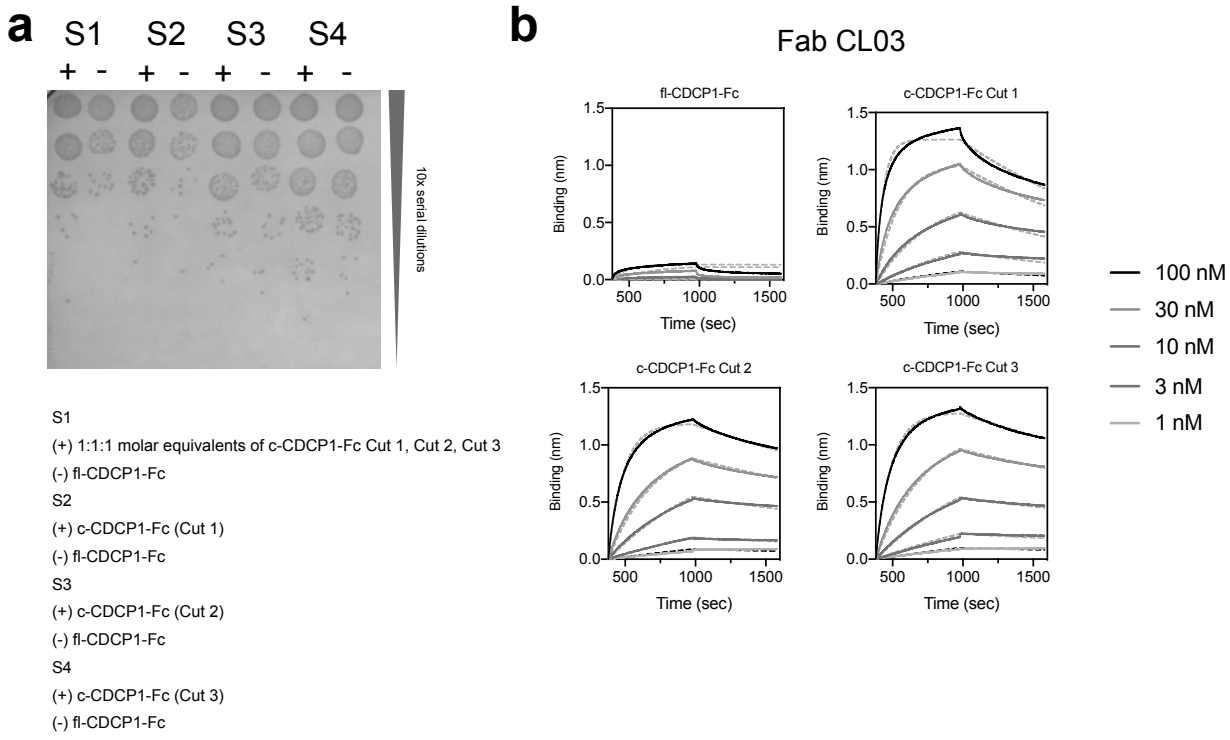

Supplementary Figure 8: Identification of cleaved CDCP1-specific Fab by phage selection. (**a**) Eluted phage from round 4 of phage selection indicate that there is enrichment for Fab-phage that recognize cleaved CDCP1 over uncleaved CDCP1. (**b**) BLI of Fab CL03 Fab binding to immobilized fl-CDCP1-Fc, c-CDCP1-Fc (Cut 1, Cut 2, Cut 3) shows that Fab CL03 selectively recognizes cleaved CDCP1 and not uncleaved CDCP1.

Supplementary Table 2: In vitro binding affinities of Fab CL03 and IgG CL03 to uncleaved and cleaved CDCP1

Ab	Antigen	K_d (nM)	k_a (sec^{-1} M^{-1})	k_d (sec^{-1})
Fab CL03	fl-CDCP1-Fc	n.d.	n.d.	n.d.
	c-CDCP1-Fc (Cut 1)	2.26 ± 0.03	(2.88 ± 0.03) x 10^5	(6.48 ± 0.05) x 10^{-4}
	c-CDCP1-Fc (Cut 2)	3.91 ± 0.02	(9.07 ± 0.03) x 10^5	(3.56± 0.02) x 10^{-4}
	c-CDCP1-Fc (Cut 3)	3.59 ± 0.02	(8.78 ± 0.03) x 10^5	(3.15 ± 0.02) x 10^{-5}
IgG CL03	fl-CDCP1-Fc	n.d.	n.d.	n.d.
	c-CDCP1-Fc (Cut 1)	0.84 ± 0.01	(6.40 ± 0.03) x 10^5	(5.35 ± 0.03) x 10^{-4}
	c-CDCP1-Fc (Cut 2)	0.37 ± 0.01	(4.73 ± 0.01) x 10^5	(1.74 ± 0.01) x 10^{-4}
	c-CDCP1-Fc (Cut 3)	0.15 ± 0.01	(4.92 ± 0.01) x 10^5	(7.43 ± 0.09) x 10^{-5}

n.d. = data not fit

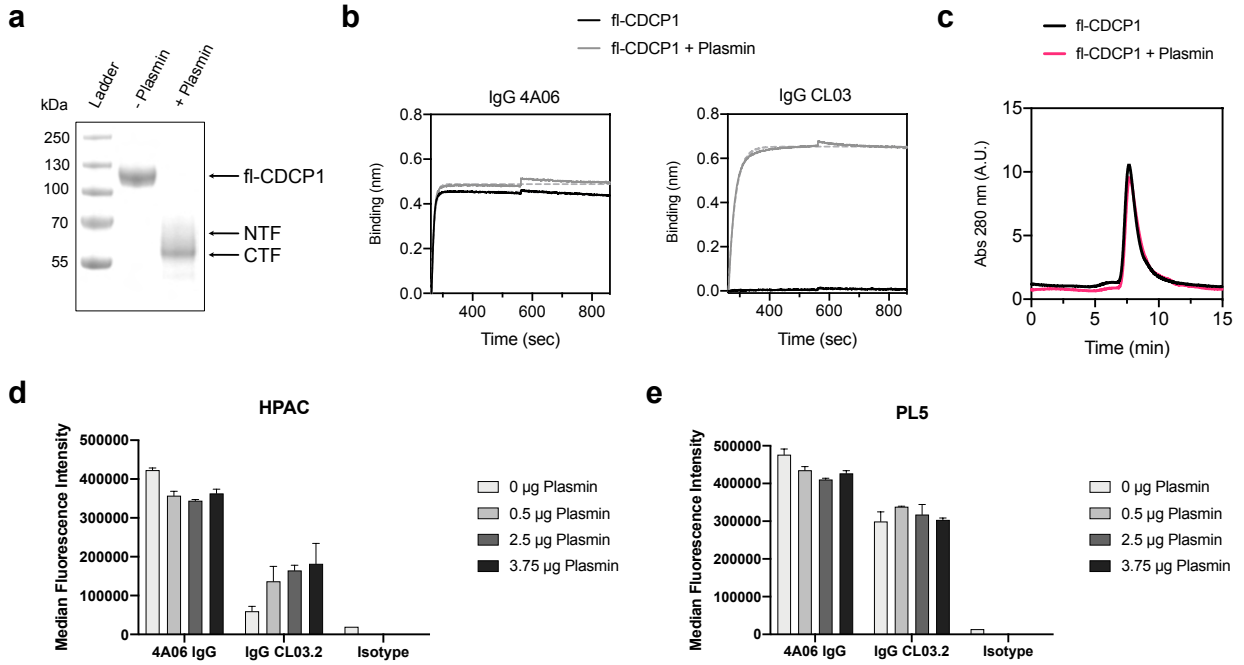

Supplementary Figure 9: IgG CL03 recognizes plasmin-cleaved CDCP1. (**a**) SDS-PAGE gel of fl-CDCP1 ectodomain treated with 0.5 µg plasmin indicates that plasmin can cleave CDCP1 at the expected molecular weights to generate c-CDCP1. (**b**) BLI of fl-CDCP1 treated with plasmin shows that IgG CL03 can specifically recognize plasmin-cleaved CDCP1. Binding of IgG 4A06 indicates that the NTF remains associated to the CTF. (**c**) SEC of plasmin-treated CDCP1 shows similar elution profiles to untreated fl-CDCP1. (**d**) Flow cytometry of HPAC cells treated with plasmin shows a dose-dependent increase in IgG CL03 binding, indicating that plasmin treatment can generate cleaved CDCP1 on the surface of HPAC cells. (**e**) Flow cytometry of PL5 cells treated with plasmin shows no additional increase in IgG CL03 binding.

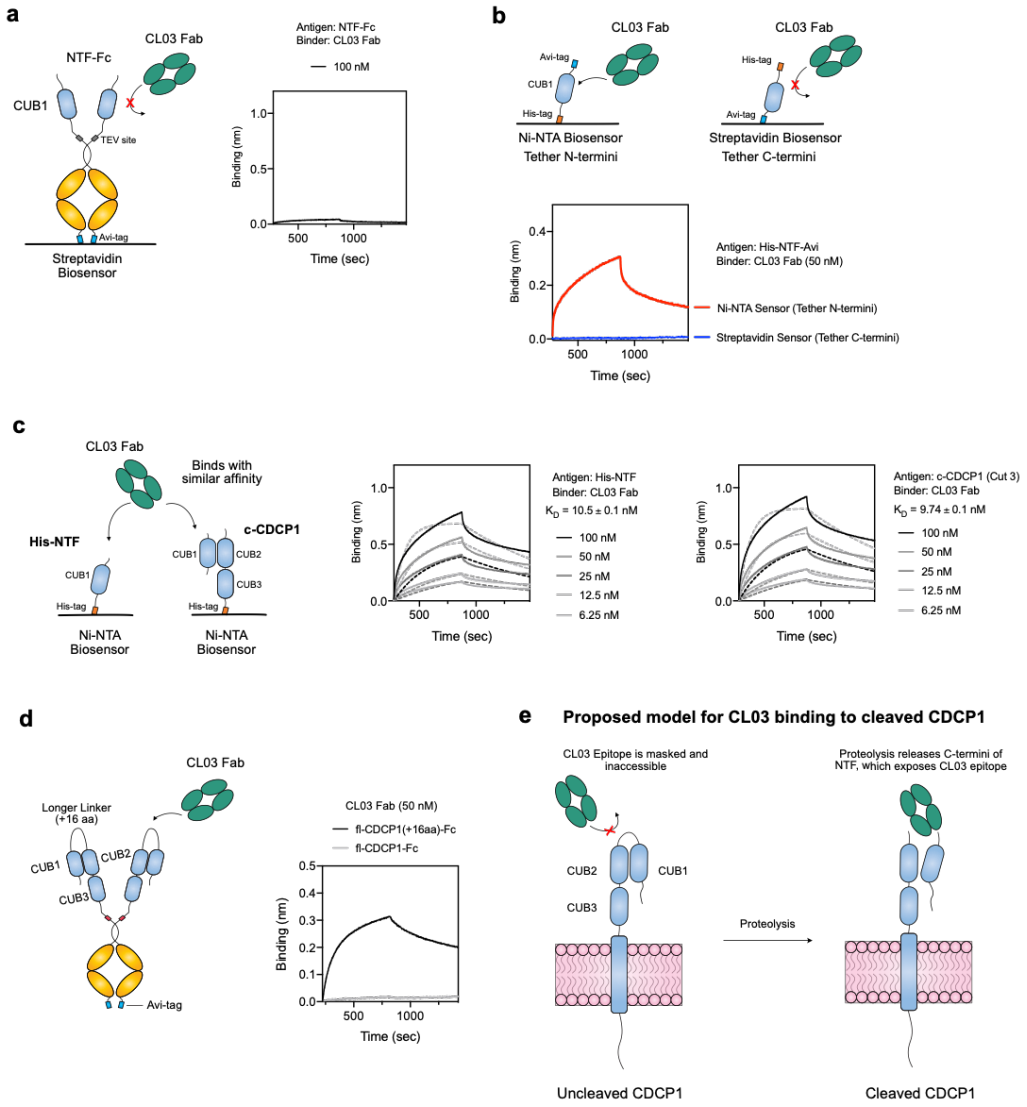

Supplementary Figure 10: CL03 binds to an epitope on the NTF that is exposed on cleaved CDCP1, but not uncleaved CDCP1. (**a**) BLI of CL03 Fab does not show binding to NTF-Fc. NTF-Fc was immobilized on a Streptavidin(SA) biosensor via a C-terminal biotinylated Avi-tag on the Fc domain. (**b**) BLI of CL03 Fab shows binding to N-terminally immobilized NTF, but not C-terminally immobilized NTF, indicating that an untethered C-termini of the NTF is necessary for CL03 binding. (**c**) Multipoint BLI show that CL03 Fab binds N-terminally tethered NTF at similar affinity to c-CDCP1, indicating the CL03 epitope is located within the NTF of CDCP1. (**d**) BLI shows CL03 Fab binding to uncleaved CDCP1 where the 2-residue R368/K369 cleavage site was replaced with a 16-amino acid linker. (**e**) Proposed model of CL03 binding to cleaved CDCP1. CL03 Fab recognizes an epitope on the NTF of CDCP1 that is masked and inaccessible when CDCP1 is uncleaved. Proteolysis releases the C-termini of the NTF and unmasks this epitope, allowing CL03 to bind and selectively recognize cleaved CDCP1 over uncleaved CDCP1.

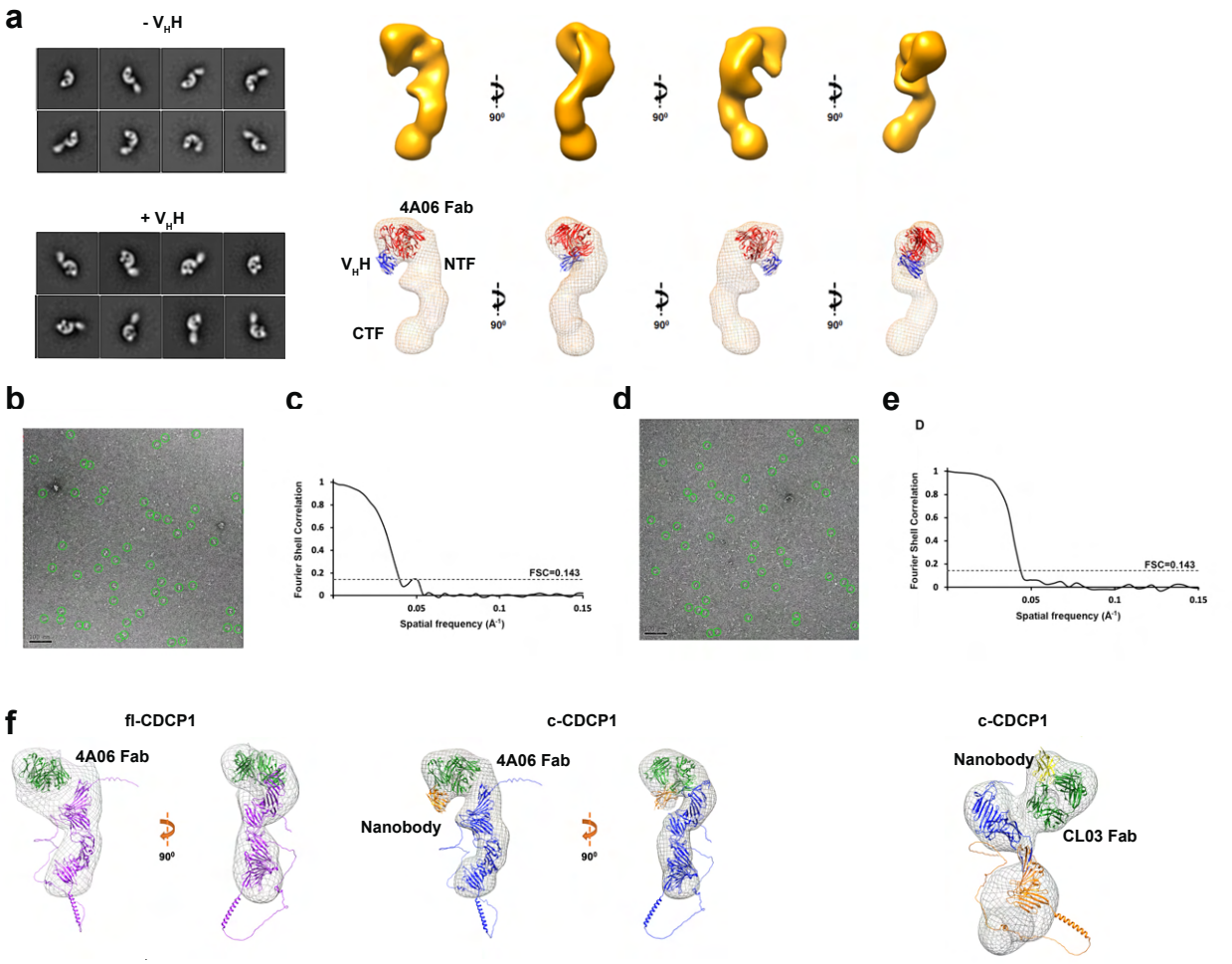

Supplementary Figure 11: Negative stain EM 3D reconstruction of cleaved CDCP1 bound to 4A06 Fab. (**a**) (*left*) 2D class averages of c-CDCP1(Cut3) + 4A06 Fab in the absence and presence of V_HH single domain antibody. (*right*) Different views of 3D negative stain EM map of c-CDCP1(Cut3) + 4A06 Fab + V_HH. Crystal structure of Fab (red) with V_HH (blue) were fitted into the 3D negative stain EM map. (**b**) A demonstrative micrograph of negatively stained c-CDCP1(Cut3) + CL03 Fab + V_HH particles. (**c**) A Fourier shell correlation plot used to determine the model resolution of 25 Å of c-CDCP1(Cut3) + CL03 Fab + V_HH, as given by 0.143 criterion. (**d**) A demonstrative micrograph of negatively stained c-CDCP1(Cut3) + 4A06 Fab + V_HH particles. (**e**) A Fourier shell correlation plot used to determine the model resolution of 23 Å of c-CDCP1(Cut3) + 4A06 Fab + V_HH, as given by 0.143 criterion. (**f**) The AlphaFold predicted model docked into the negative-stain electron microscopy maps of fl-CDCP1 (*left*) and c-CDCP1 (*middle*) bound to Fab 4A06-nanobody. The docking of the model to the EM map of c-CDCP1 bound to Fab CL03-nanobody (*right*) is less optimal, which could be due to the confirmation changes caused by Fab CL03 binding.

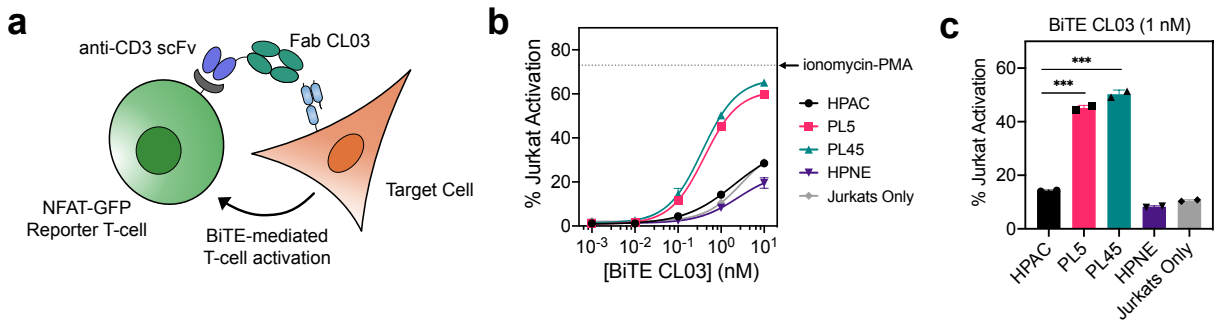

Supplementary Figure 12: CL03 as a Bi-specific T-cell engager (BiTE) can activate Jurkat cells in the presence of cleaved CDCP1-expressing PDAC cells. (**a**) Schematic of bi-specific T-cell engager (BiTE)-mediated T-cell activation assay. (**b**) Dose-dependent activation of NFAT-GFP reporter Jurkat cells above background were only observed in the presence of cleaved CDCP1-expressing PL5 and PL45 cells. (n = 2, error bars represent s.d.) (**c**) BiTE CL03 (1 nM) activates NFAT-GFP reporter T-cells in the presence of PL5 and PL45 cells but not HPAC or HPNE cells. (***p<0.001, unpaired T-test).

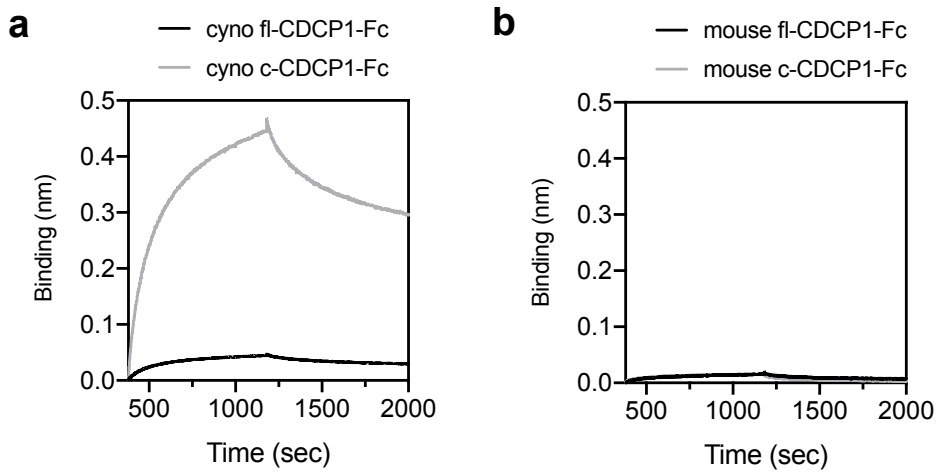

Supplementary Figure 13: Species cross-reactivity of IgG CL03. BLI of IgG CL03 to (**a**) cleaved cynomolgus CDCP1 homolog and (**b**) cleaved mouse CDCP1 homolog shows that IgG CL03 is cross-reactive and selective for cynomolgus cleaved CDCP1 but does not recognize mouse uncleaved or cleaved CDCP1.

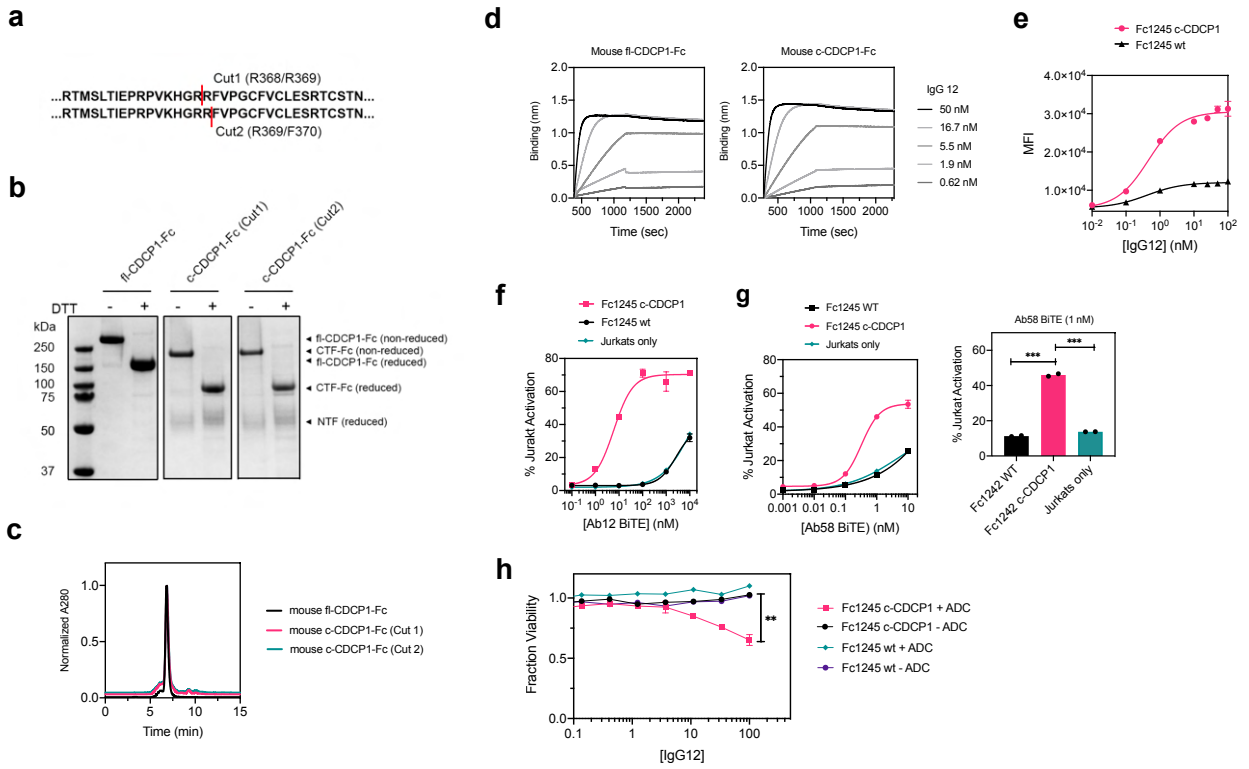

Supplementary Figure 14: Targeting mouse CDCP1 with IgG12 and IgG58. (**a**) Schematic of the two cut sites of cleaved mouse CDCP1. (**b**) SDS-PAGE gel of mouse CDCP1 antigens: fl-CDCP1-Fc, c-CDCP1-Fc (Cut 1), c-CDCP1-Fc (Cut 2) show proteins at the expected molecular weights. (**c**) SEC of mouse CDCP1 antigens: fl-CDCP1-Fc, c-CDCP1-Fc (Cut 1), c-CDCP1-Fc (Cut 2) show similar elution profiles, indicating the two fragments of cleaved CDCP1 is intact as a complex. (**d**) BLI of mouse CDCP1 antigens: fl-CDCP1-Fc and c-CDCP1-Fc show that IgG12, which recognizes the NTF of mouse CDCP1, can bind both cleaved and uncleaved mouse CDCP1, indicating that the NTF remains associated to the CTF. c-CDCP1-Fc was a 1:1 molar ratio of Cut 1 and Cut 2 antigens. (**e**) Flow cytometry shows that IgG58 binds robustly to Fc1245 c-CDCP1, and weakly to Fc1245 WT cells that express low levels of uncleaved CDCP1 (n = 3, error bars represent s.d.). (**f**) IgG12 reformatted to a BiTE shows dose-dependent activation of NFAT-GFP reporter Jurkat cells above background only in the presence of Fc1245 c-CDCP1 cells, but not in the presence of Fc1245 WT cells. (n = 2, error bars represent s.d.) (**g**) IgG58 reformatted to a BiTE shows dose-dependent activation of NFAT-GFP reporter Jurkat cells above background only in the presence of Fc1245 c-CDCP1 cells, but not in the presence of Fc1245 WT cells. (n = 2, error bars represent s.d.) (***p = 0.005, unpaired T-test) (**h**) Dose-dependent ADC-mediated cell killing with IgG12 and a secondary antibody conjugated to MMAF was only observed in Fc1245 c-CDCP1 cells and not Fc1245 WT cells. (n = 2, error bars represent s.d.) (**p = 0.0037, unpaired T-test)

Supplementary Table 3: Binding affinity of mouse CDCP1 antibodies to cleaved and uncleaved forms of mCDCP1

Ab	Antigen	K_d (nM)	k_a (sec^{-1} M^{-1})	k_d (sec^{-1})
IgG 12	fl-CDCP1-Fc	0.18 ± 0.01	(2.91 ± 0.01) x 10^5	(5.20 ± 0.10) x 10^{-5}
	c-CDCP1-Fc	0.16 ± 0.01	(2.82 ± 0.01) x 10^5	(4.54 ± 0.01) x 10^{-5}
IgG 58	fl-CDCP1-Fc	n.d.	n.d.	n.d.
	c-CDCP1-Fc	0.80 ± 0.01	(3.89 ± 0.01) x 10^5	(3.11 ± 0.06) x 10^{-5}

n.d. = data not fit

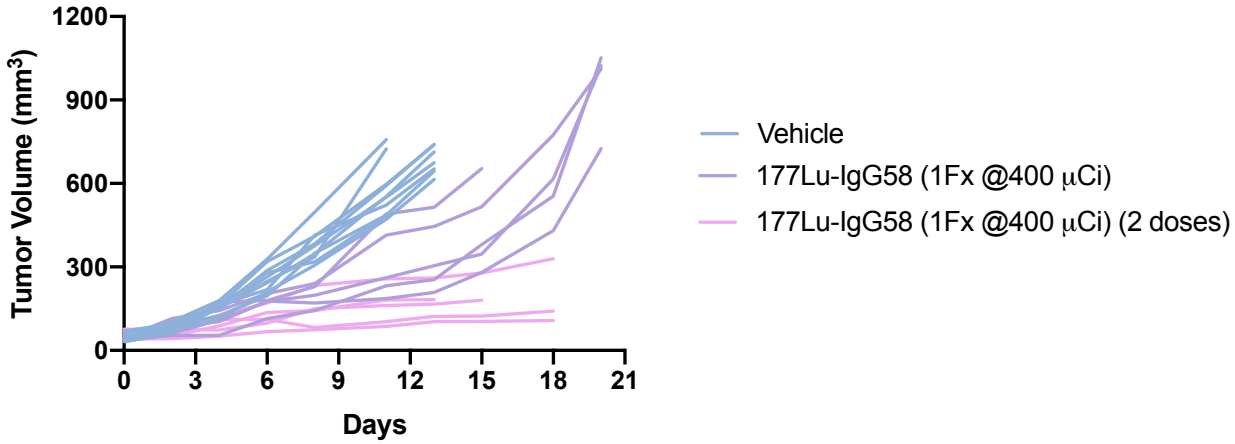

Supplementary Figure 15: Tumor volume of individual mice in ^{177}Lu-IgG58 theranostic study. Tumor volume of mice treated with vehicle or one or two 400 μCi doses of ^{177}Lu-IgG58 (n = 8 for vehicle, n = 5 per treatment arm) were monitored daily.

full unedited gel for Fig. 4D

replicate 1

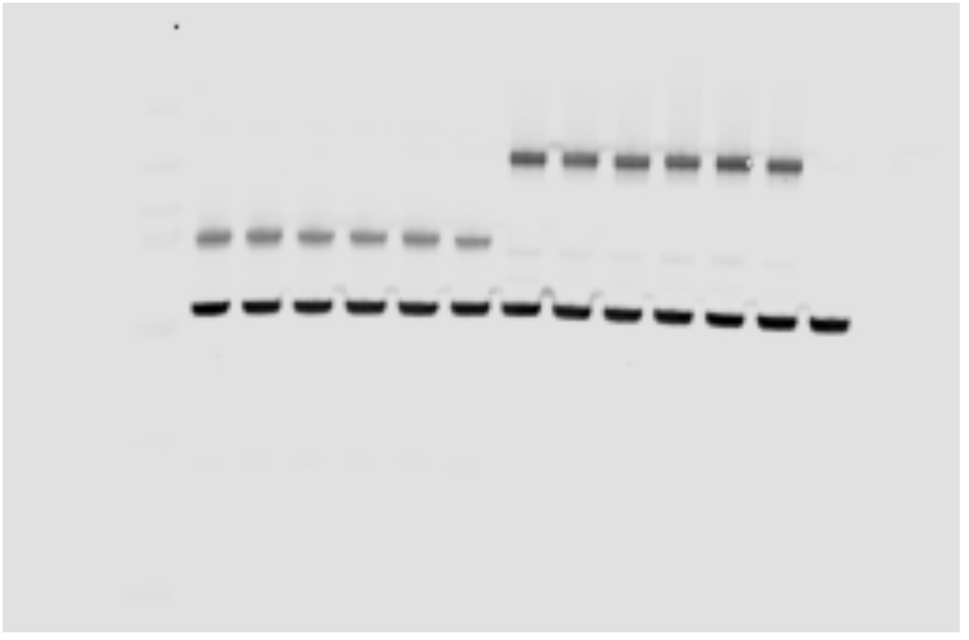

replicate 2

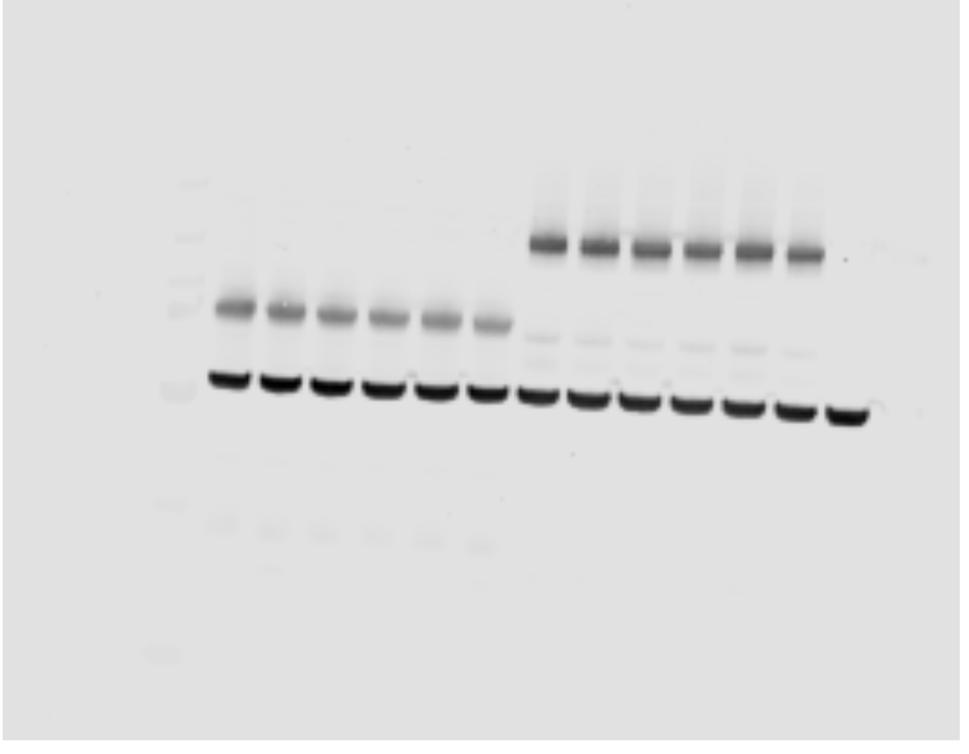

full unedited gel for Fig. 4D

replicate 1

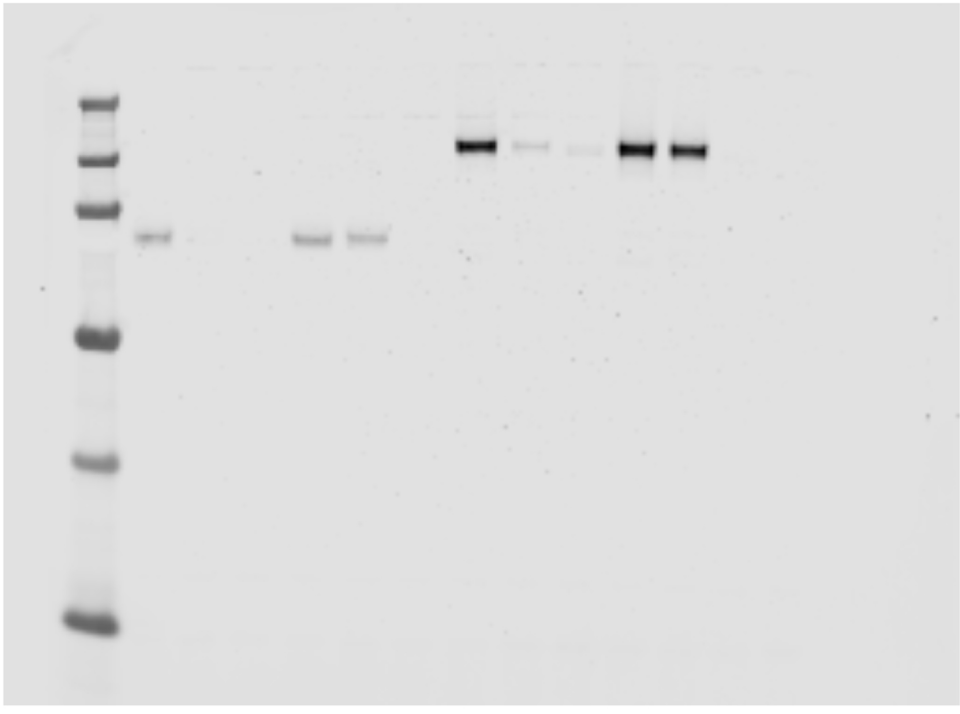

← fl-CDCP1 (pY707)

← c-CDCP1 (pY 707)

replicate 2

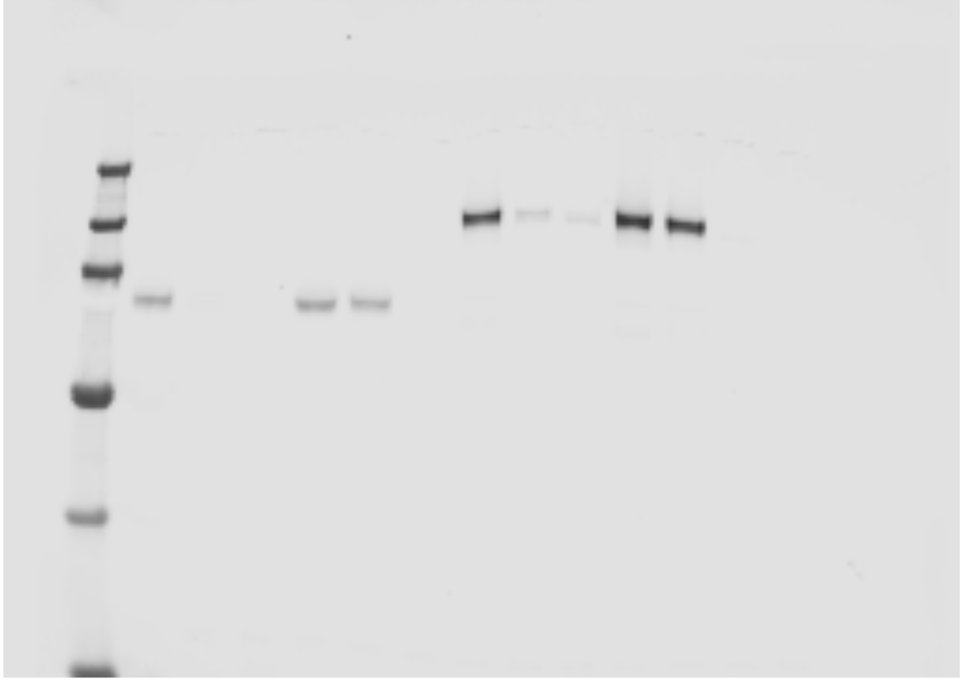

full unedited gel for Fig. 4D

replicate 1

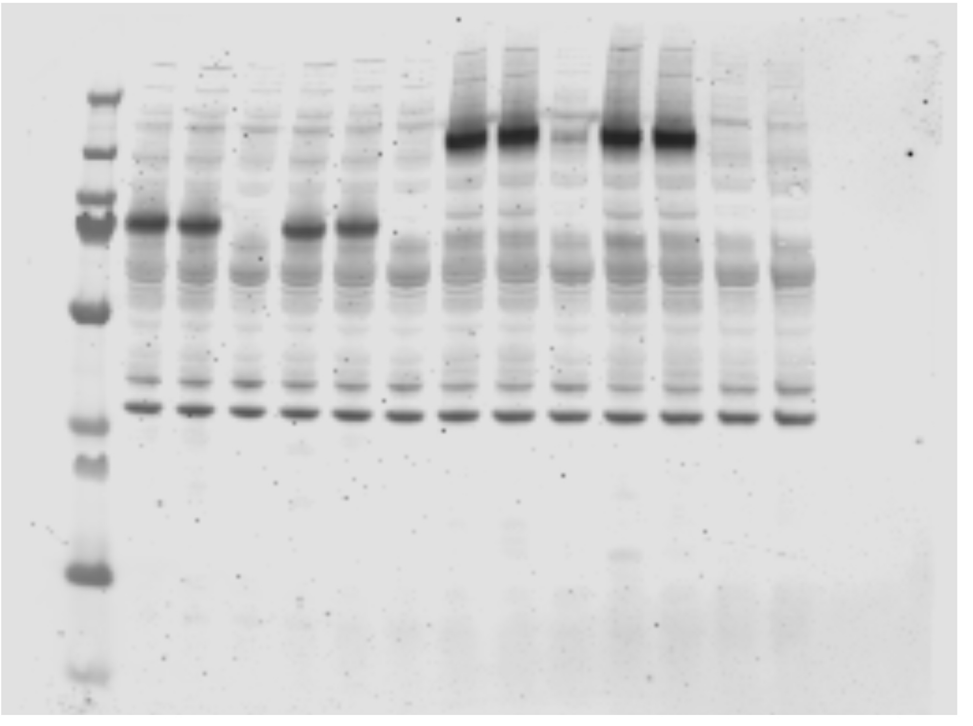

pan-pY (4G10)

replicate 2

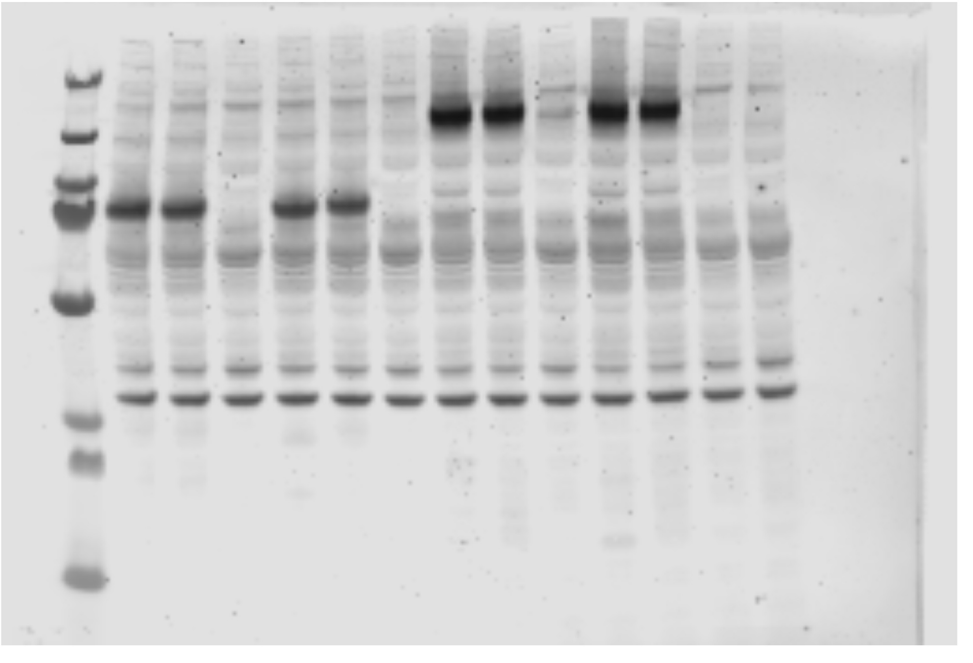

full unedited gel for Fig. 4D

replicate 1

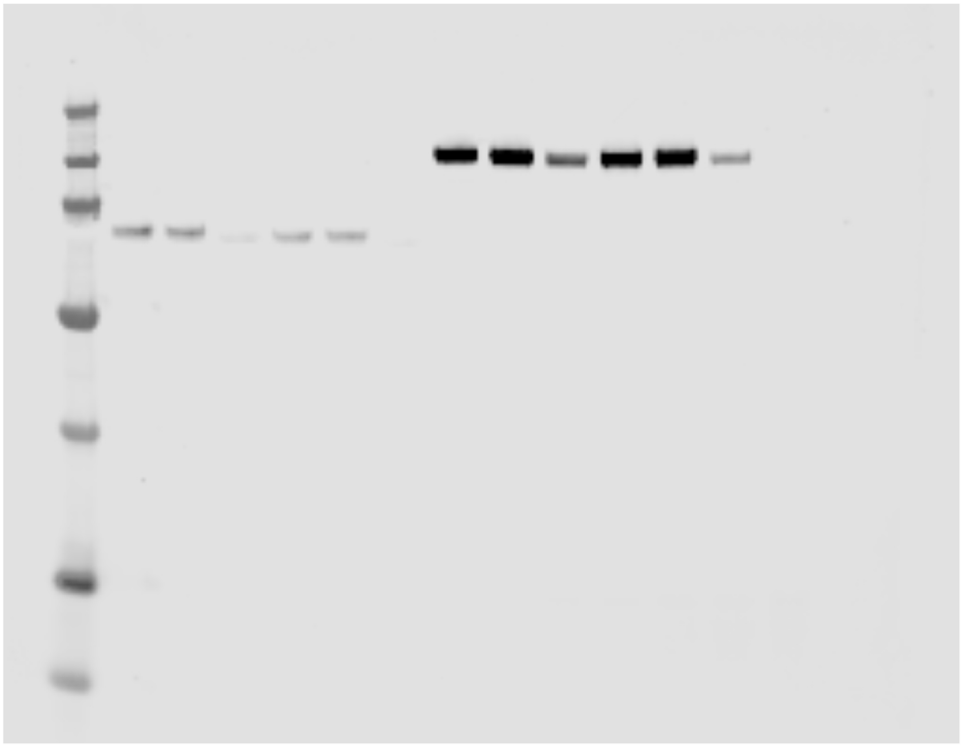

replicate 2

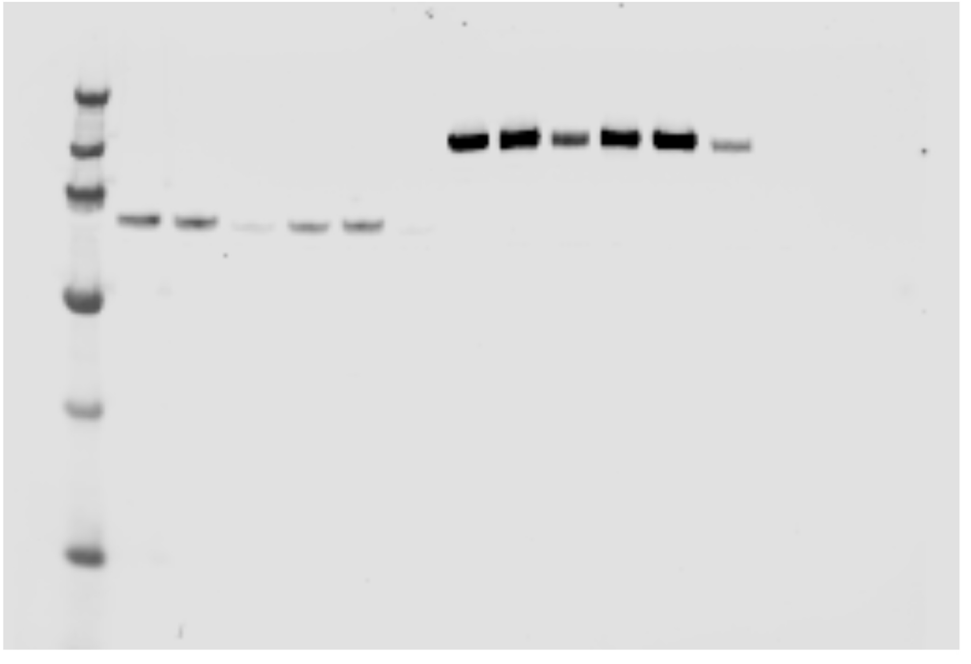

full unedited gel for Fig. 4D

replicate 1

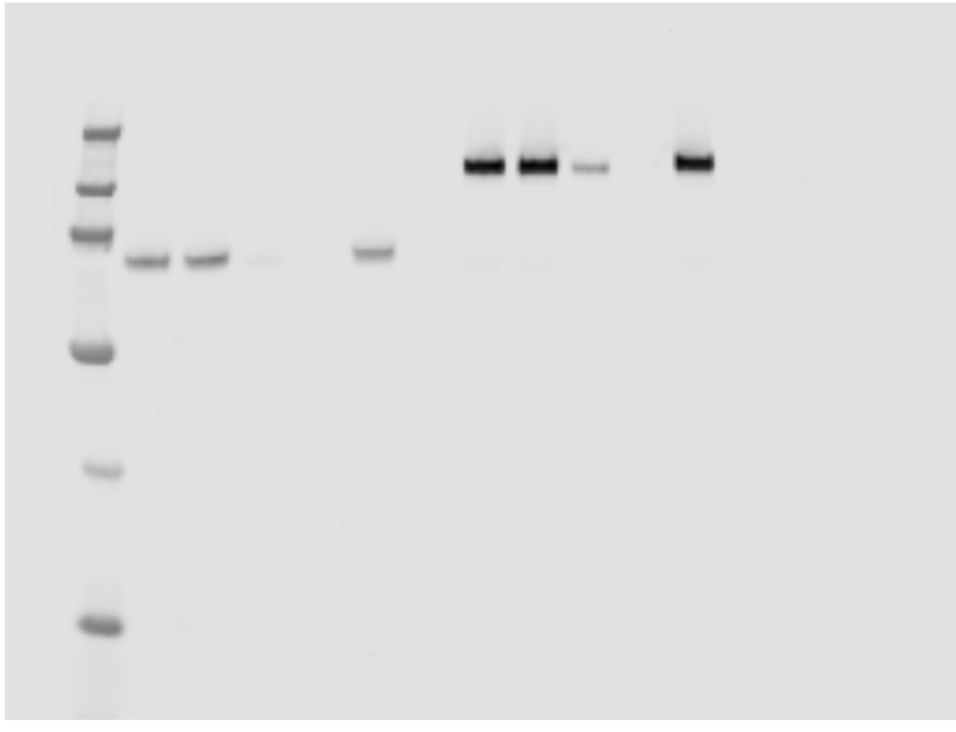

replicate 2

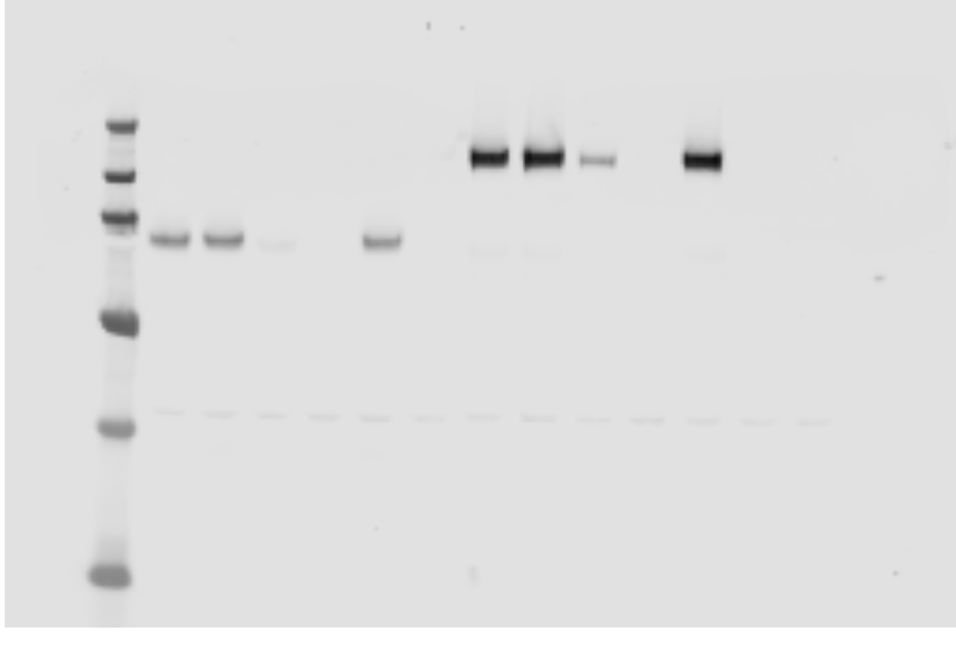

full unedited gel for Fig. 4D

replicate 1

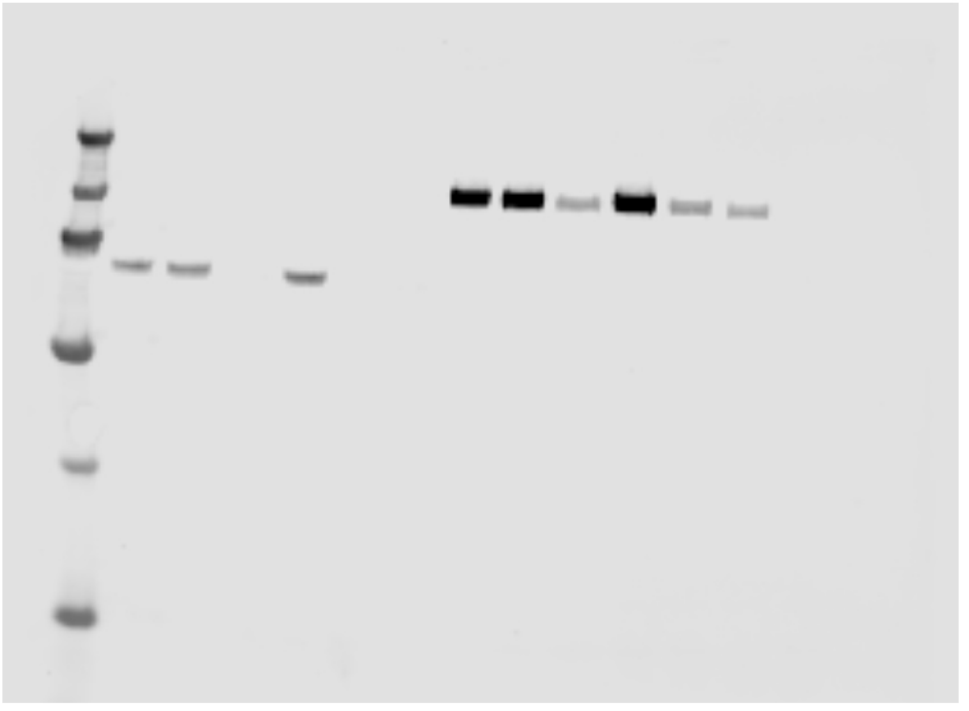

← fl-CDCP1 (pY806)

← c-CDCP1 (pY806)

replicate 2

full unedited gel for Fig. 4D

replicate 1

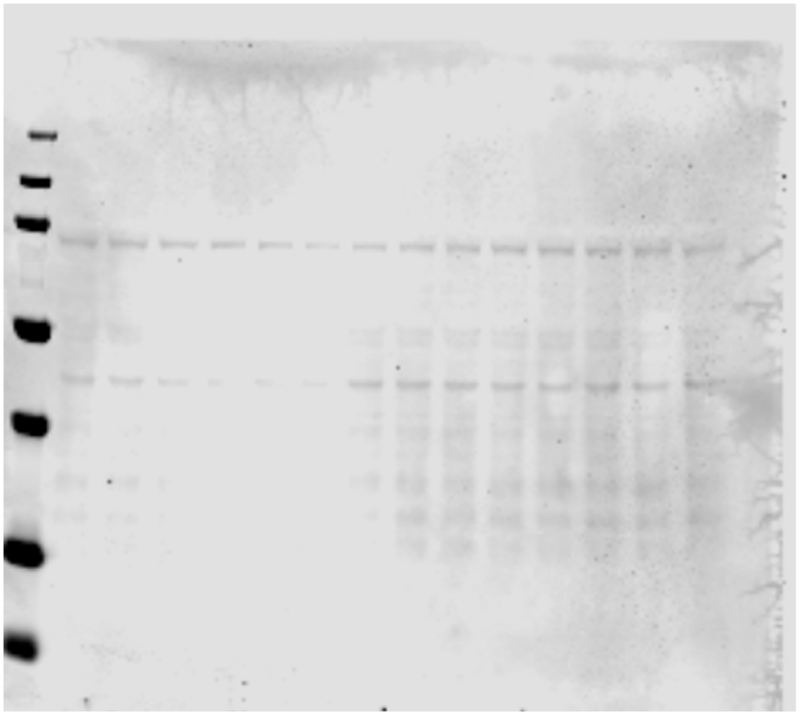

replicate 2

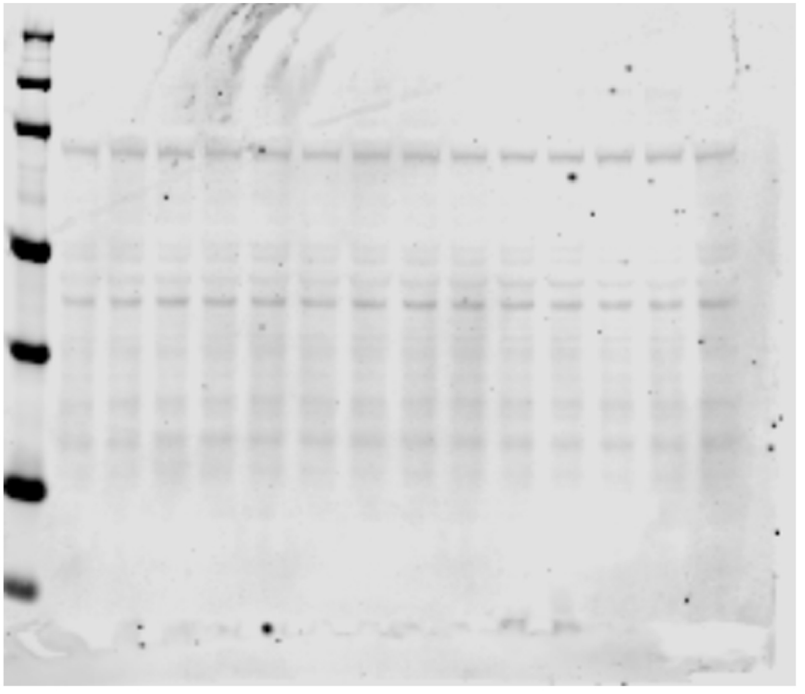

← PKCd

full unedited gel for Fig. 4D

replicate 1

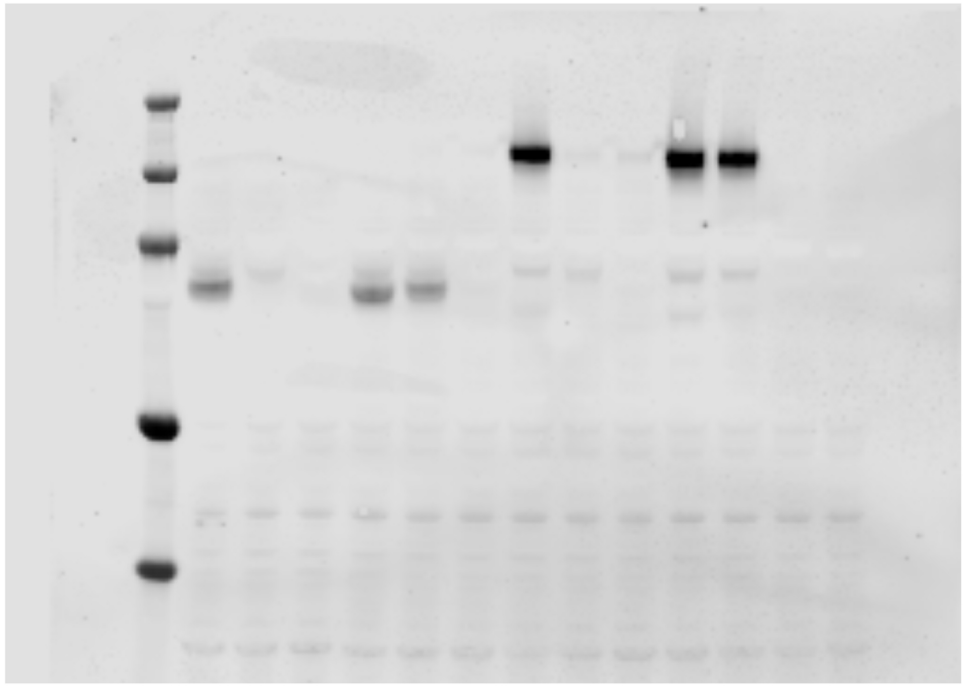

← PKCd (pY311)

replicate 2

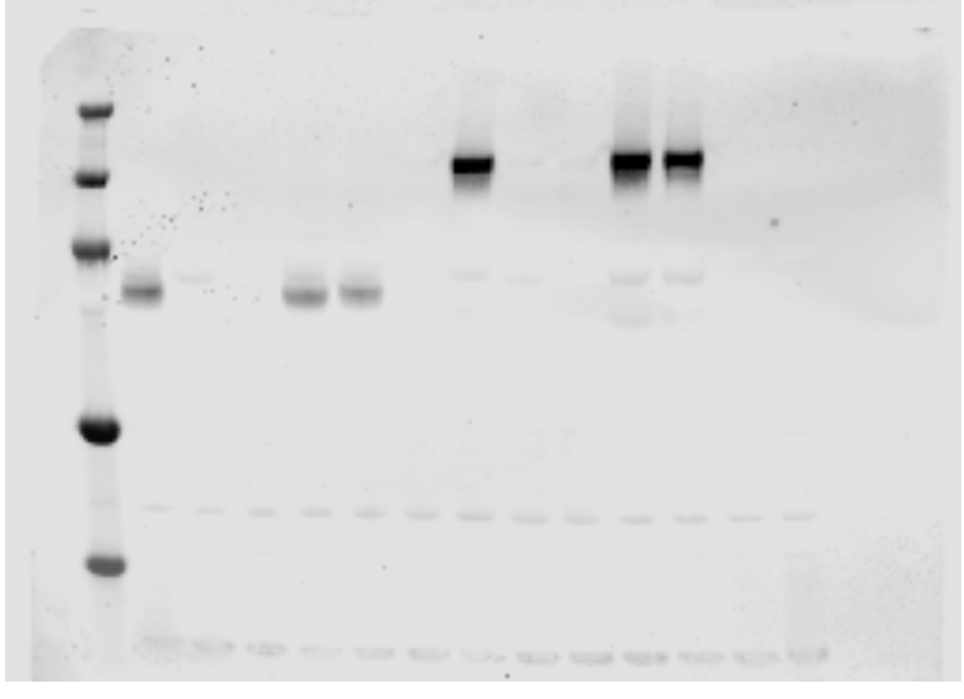

full unedited gel for Fig. 4D

replicate 1

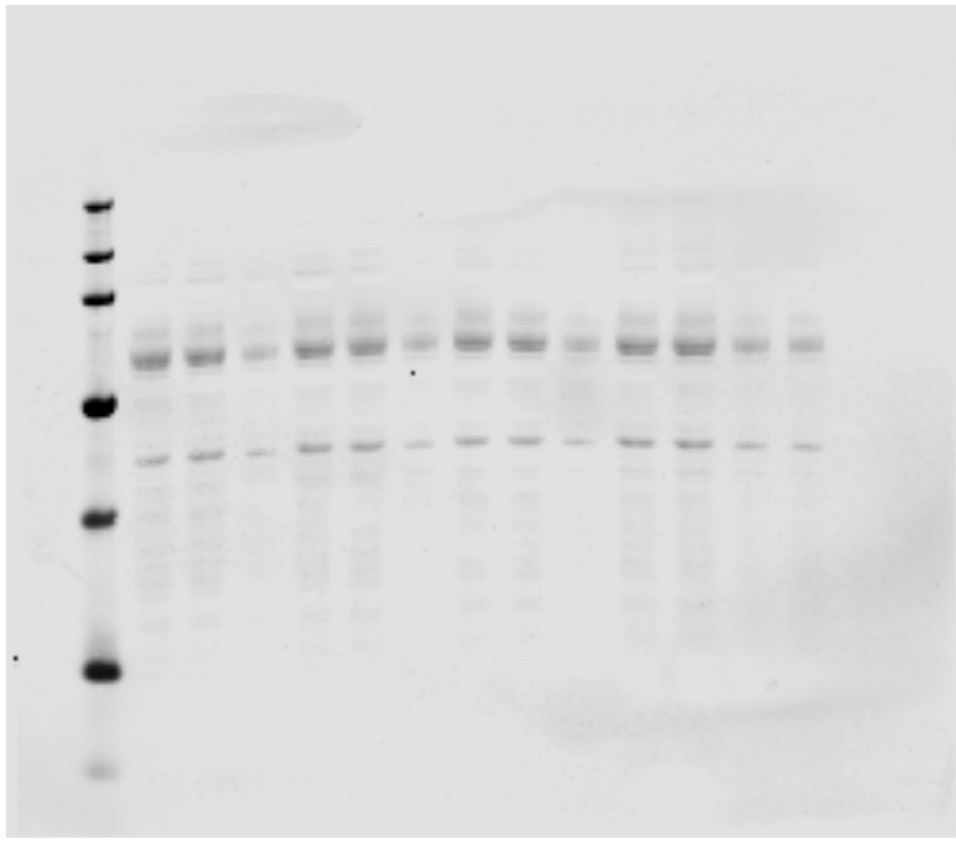

← SRC （pY416）

replicate 2

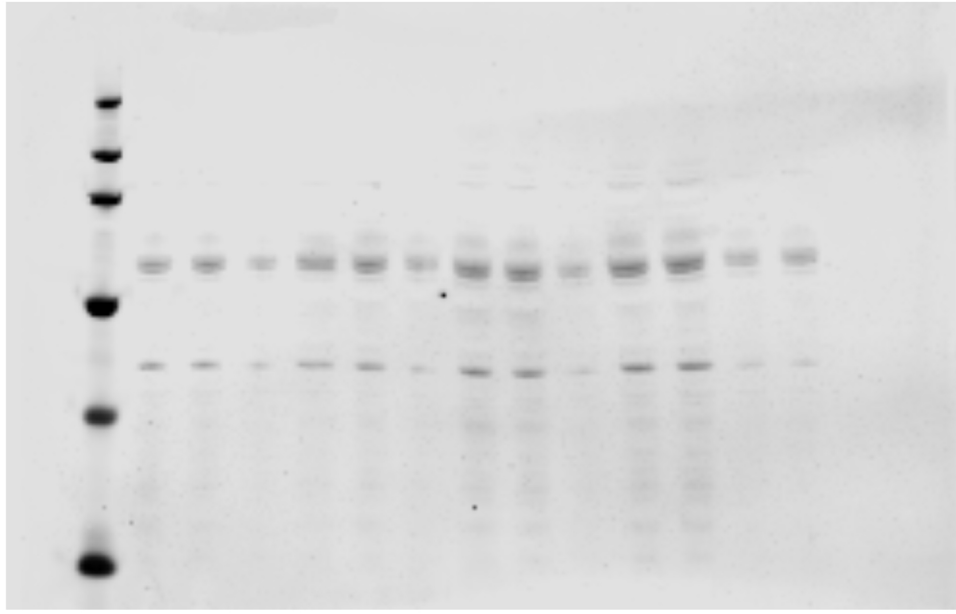

full unedited gel for Fig. 4D

replicate 1

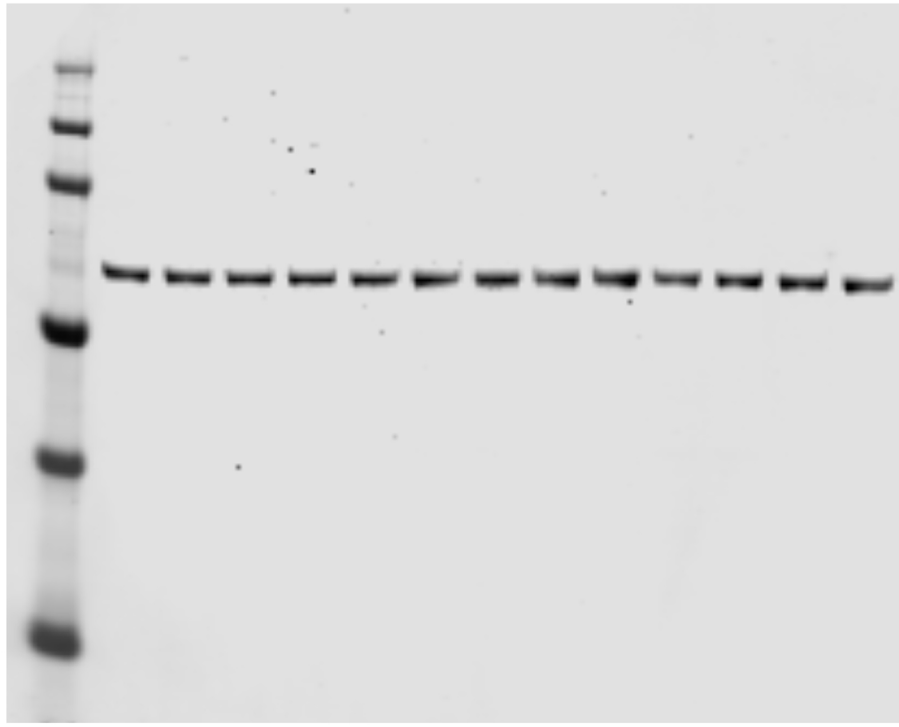

← SRC

replicate 2